Journal of Nuclear Materials 474 (2016) 105–112

Contents lists available at ScienceDirect

Journal of Nuclear Materials

journal homepage: www.elsevier.com/locate/jnucmat

Modeling solute segregation during the solidification of γ-phase U-Mo alloys

M.A. Steiner [a, *], E. Garlea [b], S.R. Agnew [a]

[a] University of Virginia, Material Science and Engineering, 395 McCormick Rd, Charlottesville, VA 22904, USA
[b] Y-12 National Security Complex, Oak Ridge, TN 37831, USA

ARTICLE INFO

Article history:
Received 21 October 2015
Received in revised form
12 February 2016
Accepted 29 February 2016
Available online 9 March 2016

Keywords:
U-Mo alloys
Solute segregation
Brody-Fleming model

ABSTRACT

Using first principles calculations, it is demonstrated that solute segregation during U-Mo solidification can be modeled using the classic Brody-Fleming limited diffusion framework. The necessary supporting equations specific to the U-Mo alloy, along with careful verification of the assumptions underpinning the Brody-Fleming model are developed, allowing for concentration profile predictions as a function of alloy composition and cooling rate. The resulting model is compared to experimental solute concentration profiles, showing excellent agreement. Combined with complementary modeling of dendritic feature sizes, the solute segregation model can be used to predict the complete microstructural state of individual U-Mo volume elements based upon cooling rates, informing ideal processing routes.

1. Introduction

A fundamental scientific concern during the processing of U-Mo alloys is their susceptibility to solute segregation during solidification, typically producing a microstructure of Mo-rich dendrites [1]. This can pose significant technical problems as it is often desirable to quench in the high-temperature body centered cubic (bcc) γ-phase of the U-Mo system, preserving both microstructural uniformity and the isotropic material properties associated with cubic phases. Under equilibrium conditions the U-Mo system experiences a eutectoid decomposition below ~570 °C from the solidified γ-phase into the non-cubic α and γ′ phases [2, 3]. The orthorhombic α-phase is particularly detrimental to the mechanical stability of the alloy due to its unique anisotropic properties, including a negative thermal expansion coefficient along one crystallographic direction [4]. Transformation kinetics through the low-temperature eutectoid region are known to be heavily dependent on the local composition [5–7]. Consequentially, solute segregation in U-Mo significantly increases the cooling rates necessary to avoid eutectoid decomposition and maintain a kinetically arrested, metastable γ-phase at ambient temperatures across the entire microstructure.

Estimating the degree of solute segregation in U-Mo resulting from solidification is important for establishing improved processing procedures and subsequent homogenization processes, especially for large samples or those with complex shapes. Utilizing first principles calculations for mass balance and diffusion, a model has been developed following the classic Brody-Fleming limited diffusion framework [8–11] to predict the profile of solute segregation in U-Mo as a function of cooling rate and microstructural feature size. The subsequent heat treatments required to homogenize U-Mo, starting from a known solute segregation profile, have already been established [12–15]. To fully predict the microstructural state created during solidification still requires a complementary model for the determination of dendrite size as a function of cooling rate and composition. Until a complete microstructural model including dendrite size can be developed, the calculations presented in the current work can be used to quickly approximate compositional profiles from the dendrite spacing found in published micrographs, which obviates the need for spatially sensitive compositional analysis.

2. Solute segregation model

The primary physical constraint in a solute segregation model is conservation of the overall alloy composition. To ensure mass balance within the alloy, the following equation must always be obeyed

* Corresponding author.
E-mail address: mas4cw@virginia.edu (M.A. Steiner).

http://dx.doi.org/10.1016/j.jnucmat.2016.02.035
0022-3115/

$$\overline{X_S} f_S + \overline{X_L} f_L = X_o \tag{1}$$

where the average composition of the solid and liquid phases, $\overline{X_S}$ and $\overline{X_L}$ respectively, are multiplied by their phase fractions in the system, f_S and f_L, and must sum to X_o, the composition of the alloy. The derivative of this equation must also hold true, so that

$$d\left(\overline{X_S} f_S\right) + d\left(\overline{X_L} f_L\right) = 0 \tag{2}$$

$$\overline{X_S}\, df_S + f_S\, d\overline{X_S} + \overline{X_L} df_L + f_L d\overline{X_L} = 0 \tag{3}$$

A second set of conservation equations regarding phase fractions are also implicit

$$f_S + f_L = 1 \tag{4}$$

$$df_S + df_L = 0 \tag{5}$$

By combining both sets of conservation relations, an alternate form of Eq. (3) can be arrived at that eliminates the liquefied phase fraction, f_L, and relates the compositions to only the solidified fraction f_S, of the system.

$$\left(\overline{X_L} - \overline{X_S}\right) df_S = f_S\, d\overline{X_S} + (1 - f_S) d\overline{X_L} \tag{6}$$

Eq. (6) is particularly useful for modeling purposes. If the interface between the liquid and solid phases of the system are in local thermodynamic equilibrium, the relationship between their instantaneous solute concentrations, $\acute{X}_S$ and $\acute{X}_L$, is known as the partition function, k, where

$$k\acute{X}_L = \acute{X}_S \text{ and } kd\acute{X}_L = d\acute{X}_S \tag{7}$$

The partition function can be determined empirically from the functional forms of the solidus and liquidus lines. Based on the U-Mo experimental phase diagram (Fig. 1) [2], both of these curves can be fitted to quadratic polynomials, yielding fits with $R^2 > 0.9995$.

$$X_L(at\%) = -0.000493\ T(^\circ C)^2 + 1.332\ T - 873.193 \tag{9}$$

$$X_S(at\%) = -0.000878\ T(^\circ C)^2 + 2.359\ T - 1539.295 \tag{10}$$

From Eqs. (9) and (10) it can be determined that the partition function for U-Mo varies between 1.676 and 1.714 as a function of temperature (Fig. 2), but can be treated as approximately constant with $k = 1.69$ across the entire compositional range, especially considering that some degree of inherent uncertainty is present within the experimental phase diagram used to fit the solidus and liquidus curves. Note that a large number of significant figures are required to ensure that the solidus and liquidus lines meet at a single temperature for the case of pure U.

With the partition function established, the relationship between X_S and X_L at the interface is known, but it is still necessary to establish the relation between the interfacial concentrations and the average concentrations to solve the conservation equation (Eq. (6)) as a function of solidification.

The simplest scenario to model is equilibrium cooling, where the rate of solidification is slow enough that the interfacial concentration of each phase will also be its average concentration [9,10], so that

$$\acute{X}_S = \overline{X_S} \text{ and } \acute{X}_L = \overline{X_L} \text{ for equilibrium cooling} \tag{11}$$

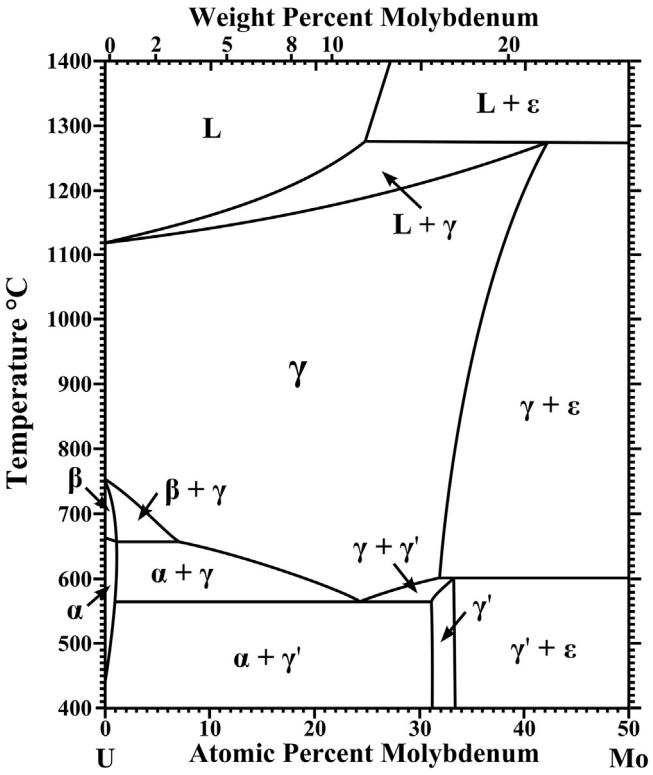

Fig. 1. Partial experimental phase diagram in the compositional range of interest, adapted from data presented in Ref. [2].

This sets up a readily solvable version of the conservation equation

$$\left(\acute{X}_L - \acute{X}_S\right) df_S = f_S\, d\acute{X}_S + (1 - f_S) d\acute{X}_L \tag{12}$$

With rearrangement, and enforcement of the boundary condition that $X_L = X_o$ when $f_S = 0$, a final solution for the interfacial concentrations during equilibrium cooling (and in this case the instantaneous average compositions) can be arrived at in terms of the solidified alloy fraction.

$$\acute{X}_L = \overline{X_L} = \frac{X_o}{(1 + (k-1) f_S)} \tag{13}$$

$$\acute{X}_S = \overline{X_S} = \frac{k X_o}{(1 + (k-1) f_S)} \tag{14}$$

In the case of equilibrium cooling there is no solute segregation present in the solid, as by definition there is no compositional variation possible within each phase.

Another scenario for solidification, known as Scheil cooling [9,10,16], occurs when diffusion is taken to be unlimited in the liquid, but no diffusion is allowed within the solid. Scheil cooling enforces the new set of equations relating the interfacial and average phase concentrations.

$$f_S\, d\overline{X_S} - \left(\acute{X}_S - \overline{X_S}\right) df_S = 0 \text{ and } \acute{X}_L = \overline{X_L} \text{ for Scheil cooling} \tag{15}$$

where the first condition ensures that changes in the average solid phase concentration are contributed strictly from the newly solidified volume, i.e. no solute can diffuse across the solid–liquid interface. The conservation relationship (Eq. (6)) for Scheil cooling

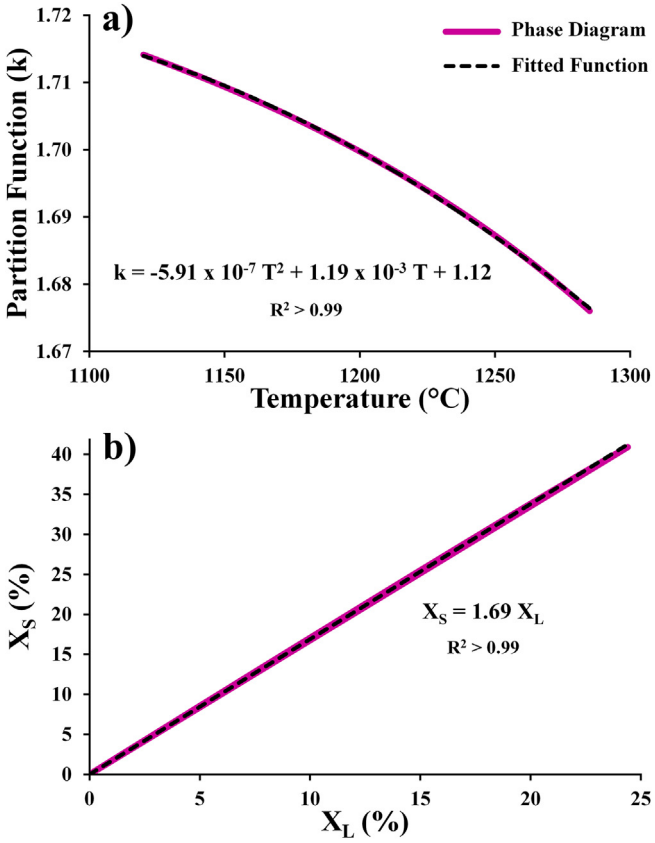

Fig. 2. **a)** The partition function as a function of temperature, utilizing the fits of Eqs. (9 &10), and **b)** A fit of the relationship of X_L vs. X_S, forcing an intercept at $X_L = X_S = 0$, to determine the most appropriate constant partition function across the entire compositional range.

reduces to

$$\left(\dot{X_L} - \dot{X_S}\right) df_S = (1 - f_S) d\dot{X_L} \tag{16}$$

After enforcing the same boundary condition as the equilibrium cooling scenario, $X_L = X_o$ when $f_S = 0$, a set of interfacial concentration equations for Scheil cooling can be derived

$$\dot{X_L} = X_o (1 - f_S)^{k-1} \tag{17}$$

$$\dot{X_S} = k X_o (1 - f_S)^{k-1} \tag{18}$$

During Scheil cooling, where no diffusion is allowed within the solid, the final solidified phase exhibits significant compositional variations as each solidified volume element inherits the concentration of the changing interface and becomes locked into place. In U-Mo alloys this leads to solute segregation of Mo to the center of the microstructural elements, which are typically dendrites. While Scheil cooling is a good first-order model of solute segregation, it is not always realistic as limited diffusion is often present within the solid phase. Improving the Scheil model to account for this limited diffusion requires a modification to Eq. (15), first proposed by Brody and Flemings [8–11], where instead of changes to the average solid phase concentration being contributed strictly from the newly solidified volume, a diffusion flux is allowed to cross the interface. This diffusion flux is determined from Fick's first law, divided by the velocity of the interface.

$$f_S \, d\overline{X_S} - \left(\dot{X_S} - \overline{X_S}\right) df_S = D_S \frac{d\dot{X_S}}{y_0} \frac{dt}{dy} \text{ and}$$

$$\dot{X_L} = \overline{X_L} \text{ for limited diffusion} \tag{19}$$

In this equation, y is the length scale of solidification, y_o is the characteristic microstructural feature size (approximately the average dendrite radius, though the move from planar to radial growth introduces a small stereological error due to curvature), and D_S is the diffusion coefficient which will follow a standard Arrhenius relationship (Eq (20)) with an activation energy for U-Mo inter-diffusion (Q) and a diffusion constant (D_o)

$$D_S = D_o e^{-\frac{Q}{k_B T}} \tag{20}$$

Utilization of this limited diffusion model requires two major approximations. 1) The diffusion coefficient can be treated as a constant, with no dependence on temperature or composition occurring during the transformation. 2) The concentration gradient over the whole solid phase may be approximated at any time by the gradient near the interface. With these approximations, the conservation relationship for the case of limited diffusion becomes

$$\left(\dot{X_L} - \dot{X_S}\right) df_S = \frac{dt}{dy} \frac{D_S}{y_o} d\dot{X_S} + (1 - f_S) d\dot{X_L} \tag{21}$$

Growth of the solid phase will be a diffusion limited process as the liquid and solid phases share different compositions. Therefore the length scale of solidification can be expected to follow a parabolic relationship with time, so that

$$y^2 = \lambda t \text{ where } \lambda = \frac{y_o^2}{t_o} \tag{22}$$

λ is a constant and can therefore be determined from the total time required for solidification, t_o, and the distance the solidification occurred over, y_o. Taking the derivative of Eq. (22), and employing the definitional relationship that $y = f_S y_o$, it can be established that

$$\frac{dt}{dy} = \frac{t_o}{y_o} 2 f_s \tag{23}$$

This allows the relationship in Eq. (21) to be rewritten in a form than can be more readily integrated

$$(1 - k) \dot{X_L} \, df_S = (1 + (\alpha k - 1) f_S) d\dot{X_L} \text{ where } \alpha = 2 \frac{D_S t_o}{y_o^2} \tag{24}$$

and solved for the boundary condition $\dot{X_L} = X_o$ when $f_S = 0$, yielding

$$\dot{X_L} = X_o (1 + (\alpha k - 1) f_S)^{\frac{(1-k)}{(\alpha k - 1)}} \tag{25}$$

$$\dot{X_S} = k X_o (1 + (\alpha k - 1) f_S)^{\frac{(1-k)}{(\alpha k - 1)}} \tag{26}$$

When $\alpha = 0$ these equations reduce to the case of Scheil cooling, and when $\alpha = 1$ they reduce to the equilibrium cooling equations. As a result, both Scheil and equilibrium cooling are simply special cases of the limited diffusion equations. In scenarios that $\alpha > 1$, the solutions for the Brody-Fleming limited diffusion condition (Eq. (19)) become non-physical and require a correction [11], but this is not of concern for any systems experiencing solute segregation as they do not approach equilibrium ($\alpha \geq 1$) conditions. The behavior of interfacial concentrations as a function of solidified fraction can be seen in Fig. 3.

Solutions to the conservation relationship provide instantaneous concentrations at the interface, not the final compositional profile after solidification. Unlike the Scheil and equilibrium cooling cases, where it is easy to establish the final concentrations within the alloy as a function of solidified percentile as either all or none of the solute is mobile, solutions involving limited diffusion in the solid phase require additional calculations. It is easiest to model the final concentration profile in the solid by breaking solidification into finite time steps and estimating the diffusion of solute from the solid back into the liquid through numerical methods. Solute mass must be conserved between the liquid and solidified regions at any given time. Any surplus in solute mass acquired by the liquid during the time step must have diffused to the interface from the previously solidified elements. As the concentration gradient is approximately constant, this surplus solute mass can be divided equally and subtracted from each previously existing solid element. This simple numerical solution allows for final solute segregation profiles to be computed for limited diffusion cases for an established α parameter (Fig. 4). The resulting final concentrations profiles in the solid phase are predominantly linear in regard to their solidified percentile until $\alpha < 0.2$, after which curves begin to bow and more closely resemble the Scheil cooling ($\alpha = 0$) profile.

These numerical solutions rely, as previously mentioned, on two critical approximations that must be examined for U-Mo. The first was that the diffusion coefficient can be treated as a constant in regard to temperature. In reality, D_s will be dependent on both solute concentration and temperature, which are both functions of the solidified fraction. The relationship between concentration and diffusion for the U-Mo γ-phase was first established by Adda et al. [17, 18]. More recent diffusion studies have largely preserved the diffusion coefficients of these early findings, but have revised some anomalies in the concentration dependencies of Q and D_o, making them easier to fit as simple functions [19].

$$Q(kJ) = 14.635 \ln(Mo\ at\%) + 137.54 \tag{27}$$

$$\ln\left(D_o\left(m^2/s\right)\right) = -0.0725\ (Mo\ at\%) - 12.463 \tag{28}$$

With these equations and the concentration–temperature relationship provided by the liquidus line (Eq. (9)) of the system, the average diffusion coefficient ($\overline{D_S}$) of the solid phase can be calculated as a function of the solidified fraction of the sample. The average concentration of Mo in the solid phase will decrease along with temperature during solidification in the U-Mo system under any cooling condition due to the nature of the phase diagram. This is fortuitous, as the increased diffusion rates expected at elevated temperatures near the beginning of solidification are offset by the higher activation energies for inter-diffusion (Q) at Mo-rich compositions, leading to relatively constant diffusion coefficients across the entire solidification range. Average diffusion coefficients as a function of solidification for the cases of Scheil and equilibrium cooling are plotted for both U – 5 wt% Mo (11.5 at%) and U – 10 wt% Mo (22 at%) in Fig. 5, and the curves for limited diffusion cases will rest between these two bounds. For all but the most extreme cases (e.g., below 5 wt% Mo it becomes very hard to avoid the formation of the α-phase when cooling through the eutectoid region [5, 6]), the average diffusion coefficient does not vary during solidification by more than a factor of two, and at compositions near the eutectoid that experience solute segregation (the cases of interest to many current researchers) diffusion rates are expected to be nearly constant.

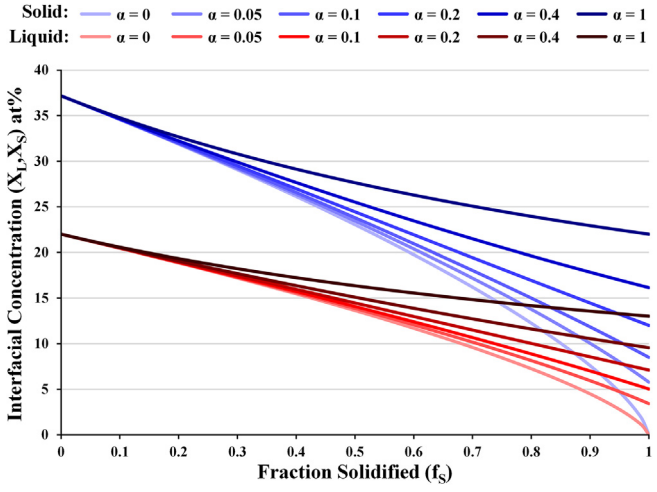

Fig. 3. Interfacial concentrations of the liquid and solid phases as a function of solidified fraction, starting from U – 10 wt% Mo (22 at%). In the extreme of $\alpha = 1$ the concentrations are the equivalent of the equilibrium cooling condition, and at $\alpha = 0$ they are representative of Scheil cooling, with no diffusion in the solid.

The second assumption made in the limited diffusion model is that the concentration gradient over whole solid may be approximated at any time by the gradient at the surface. This can quickly be assessed in a qualitative manner by noting that the second derivatives of the curves in Fig. 4, i.e. changes in slope and in this case the concentration gradients present at $f_S = 1$, only vary significantly in cases approaching Scheil cooling. Quantitative calculations of the instantaneous gradients confirm that the approximation only falls apart in the cases where $\alpha < 0.1$. While the approximation no longer holds for very low α values, the errors contributed to the model in this regime will be inherently low because diffusion is negligible and the concentration gradient becomes irrelevant.

3. Results & discussion

Two sources providing spatially sensitive compositional analysis of U-Mo in solute segregated conditions are available to verify the limited diffusion model [7, 15]. In both cases, the analysis was conducted in a scanning electron microscope by energy dispersive X-ray spectrometry (EDS). As volume elements with less solute will always have solidified later in the freezing process, the cumulative distribution function of local concentrations will be the same as the final concentration profile as a function of the solidified percentile, allowing a ready means of conversion from the concentration maps presented in Refs. [7, 15] (Appendix A).

The first of these references presents concentration maps of as-cast U – 5 wt% Mo, U – 7 wt% Mo, and U – 10 wt% Mo alloys [7], cooled at a rate of approximately 0.5 °C/s. The second reference provides a concentration map and cumulative distribution function for a U – 10 wt% Mo sample that was chill cast (arc-melted into a copper mold) at an unknown rate [15]. Based upon the fine dendritic structure (~8 μm inter-dendritic spacing) and comparison to samples produced in induction furnaces, which typically exhibit inter-dendrite distances on the scale of 25–100 μm [7, 20] from cooling rates around 0.5 °C/s [7, 21], the cooling rate of the chill cast sample is expected to be significantly above 1 °C/s. Fig. 6 presents the experimental concentration profiles obtained from these two studies, along with the profiles generated from the limited diffusion model (e.g. curves in Fig. 4) that produce the best fits. All of the profiles exhibit a small dip in concentration from the expected form of the profile in their very last solidified elements. This can be explained by the growth fronts of dendrites coming into contact as f_s approaches 1, lowering the amount of solid–liquid interfacial area and limiting the amount of Mo solute diffusion out of the solid and into remaining liquid relative to the previous solidified

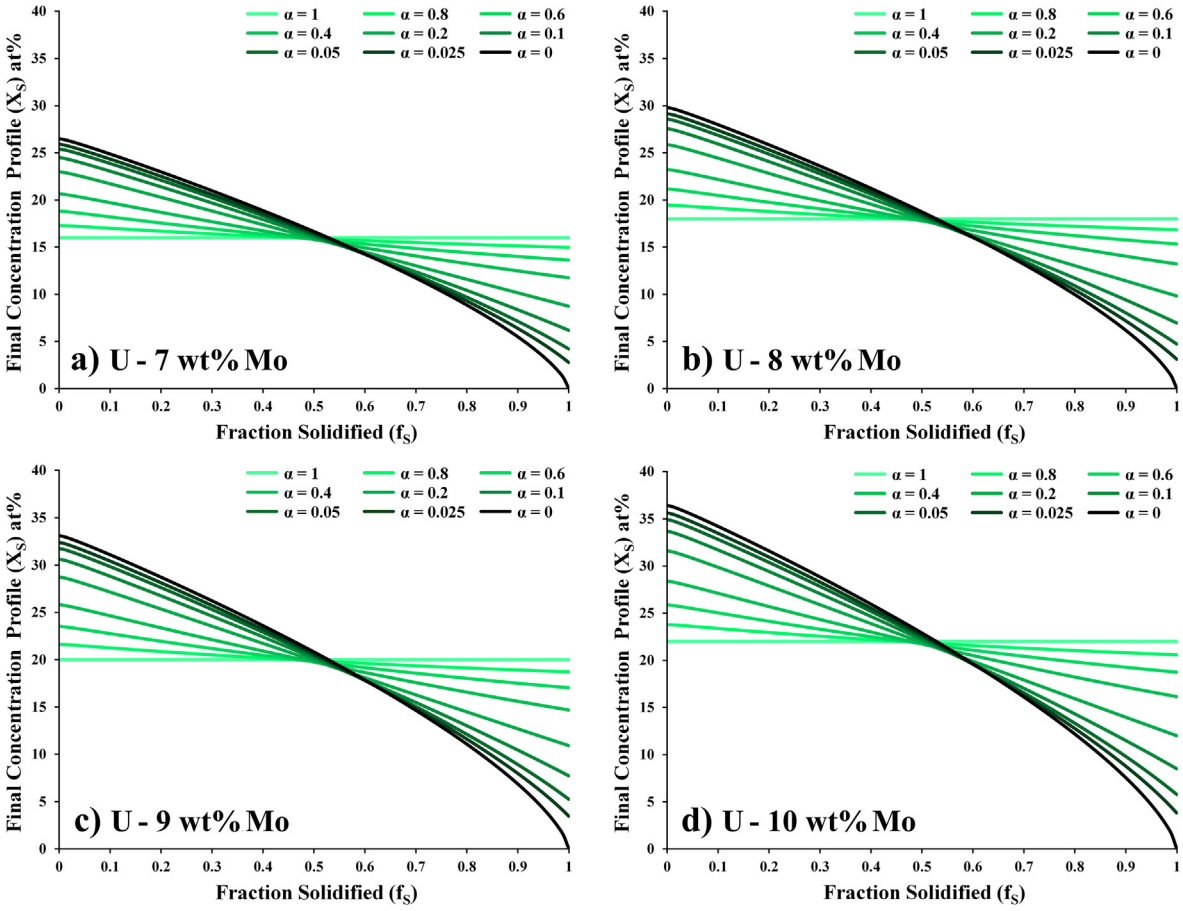

Fig. 4. Final concentrations profiles of the solid phase as a function of solidified percentile and a number of different α conditions for **a)** U − 7 wt% Mo (16 at%) **b)** U − 8 wt% Mo (18 at%) **c)** U − 9 wt% Mo (20 at%) **d)** U − 10 wt% Mo (22 at%).

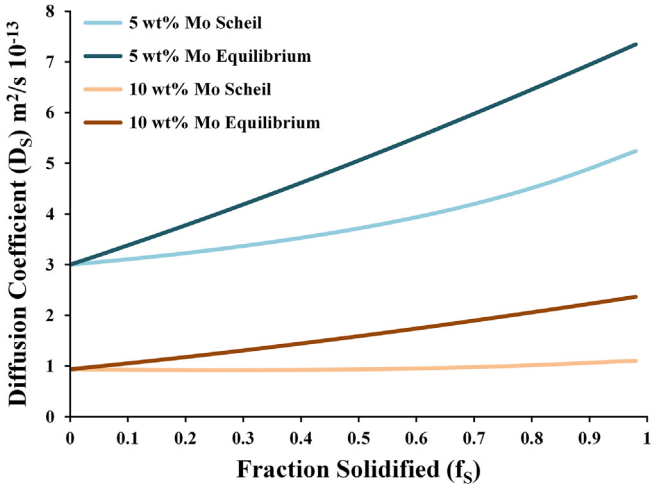

Fig. 5. Average diffusion coefficients, $\overline{D_S}$, experienced in the solid phase as a function of solidified fraction for both U − 5 wt% Mo (11.5 at%) and U − 10 wt% Mo (22 at%) under equilibrium and Scheil cooling conditions. Limited diffusion cases will exists between these two bounds.

elements.

The experimentally measured average alloy compositions in Fig. 6 are presented in Table 1, along with the α parameters of the model profiles, the calculated average diffusion constants, and temperature ranges covered during solidification based upon the α parameter and composition. The approximate average dendrite radius for each sample is also listed, determined from micrographs presented in each reference. From the definition of α in Eq. (24) and the information provided in Table 1, it is possible to make an estimate on the expected cooling rates to compare with the reported values. The model based prediction of 0.3 °C/s is close to the reported ~0.5 °C/s (over a large temperature range) reported for the samples in Refs. [7], and it is possible that the slightly slower rate is related to the latent heat of solidification released during solidification, which will slow the transformation relative to the general approximation of $dT/dt = \Delta T/t_0$. While the rate of cooling for the sample in Ref. [15] is unknown, the 4.6 °C/s predicted by the model is consistent with expectations for chill casting. In summary, all of the available data appears to support application of the Brody-Fleming limited diffusion model and the alloy specific equations provided in this paper to the U-Mo system.

The solidified U-Mo γ-phase is not the equilibrium phase at ambient temperatures and solute concentration has a large impact on the cooling rates required to transverse the eutectoid region without precipitating the undesirable, highly anisotropic α-phase. From the equilibrium phase diagram (Fig. 1) it is already clear that the α-phase becomes stable at higher temperatures for Mo-lean compositions. Time-Temperature-Transformation (TTT) diagrams for U-Mo exhibit the classic transformation nose behavior [5, 6], where the transformation is limited by the smaller driving forces present at high temperatures, while at lower temperatures the transformation is limited by slower inter-atomic diffusion. In order

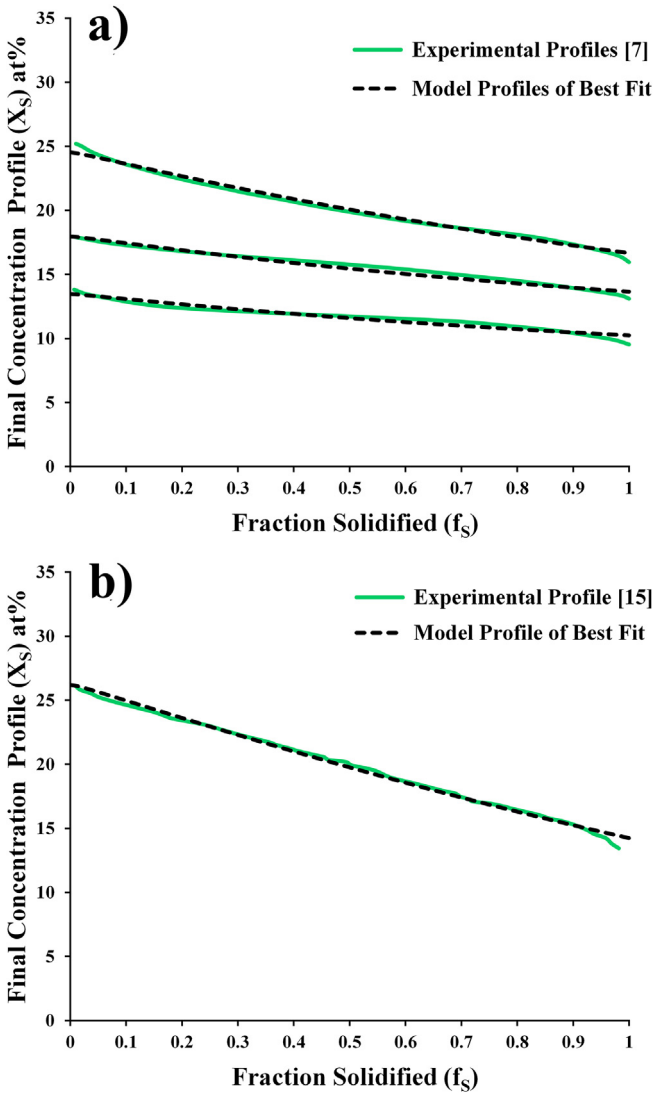

Fig. 6. Experimentally determined final concentrations profiles of the solid phase as a function of solidified percentile along with fitted model predictions, for samples of **a)** U − 5 wt% Mo, U − 7 wt% Mo, and U − 10 wt% Mo [7] and **b)** chill-cast U − 10 wt% Mo [15].

to quench in the meta-stable cubic γ-phase, and avoid creating the U-rich α-phase, the goal is therefore to cool fast enough to avoid crossing the nose of the TTT diagram, at which point the γ-phase will be preserved by the limited diffusion available at ambient temperatures to overcome the nucleation barrier of a precipitate's interfacial energy. While there is some small disagreement as to the exact form of the U-Mo TTT diagrams across the compositional range, the previous studies unanimously confirm that the quench rates necessary to avoid formation of the deleterious α-phase increase dramatically with lower Mo content. It has been experimentally verified that Mo-lean regions within a microstructure form the α-phase first via eutectoid decomposition, and the eutectoid phases will generally nucleate on a grain boundary, where the nucleation energy required is the lowest due to the existing interface, before expanding out through the Mo-lean regions and later through the entire microstructure as the nucleation barrier for the phase transformation has already been overcome and the γ-phase is not in energetic equilibrium.

The parameter of greatest concern in U-Mo segregation is the solute concentration of the very last solidified elements of the microstructure, which will have the both lowest solute content and are located along the grain boundaries that provide ready nucleation sites for the eutectoid decomposition. The solute concentration of the last solidified element as a fraction of the average alloy composition turns out to independent of the average alloy composition for a given α parameter. A graph of this ratio as a function of α is presented in Fig. 7. A researcher with a U − 20 at% Mo alloy wishing to ensure that no local solute concentration in the microstructure falls below U - 18 at% Mo (90% the average) could infer from this chart that $\alpha > 0.7$ would be necessary in their cooling procedure. It is worth noting that the small dip in concentrations observed in the last solidified elements of experimental profiles (Fig. 6) suggests that the actual concentration at some points of the boundary may be approximately 1 at% Mo below the model prediction.

Determining the α-parameter for a given alloy and cooling rate is complicated by the relationship between the average dendrite size (and thusly y_o) and the cooling rate during solidification, both of which impact the α-parameter. The primary inter-dendrite

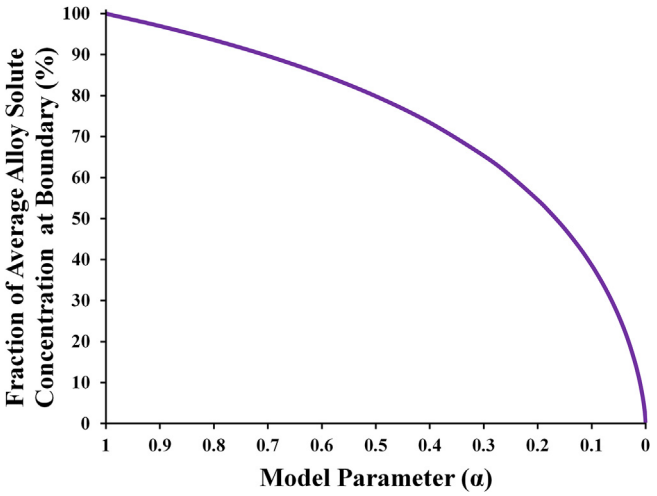

Fig. 7. Solute concentration of the last solidified element as a fraction of the average alloy composition as a function of the cooling rate dependent α-parameter.

Table 1
Average experimentally determined atomic concentrations, dendrite radii, cooling rates, and the fitted α parameters used in Fig. 6. Combined with the calculated average diffusion coefficients and the temperature ranges covered during solidification, the presented model is able to make estimates on the cooling rates that compare well to reported values.

Source	Nominal wt%	At %	α	Cooling rate (°C/s)		D_s (10^{-13} m^2/s)	Solidification ΔT (°C)	Avg. Dendrite radius (μm)
				Reported	Model			
[7]	5	11.7	0.54	~0.5	0.3	4.67	35.64	~15
[7]	7	15.6	0.65	~0.5	0.3	2.77	53.57	~12
[7]	10	20.3	0.65	~0.5	0.3	1.62	82.71	~12
[15]	10	20	0.38	>1	4.6	1.56	89.36	~4

spacing (λ) for many materials can be approximated as a function of cooling rate by

$$\lambda = m\left(\dot{T}\right)^{n} \tag{29}$$

where m and n are experimentally determined constants [10]. Consequentially, if these experimental constants were to be established for the U-Mo system, it would be possible to predict the complete microstructure of each volume element including dendrite size and solute segregation if given the average alloy composition and the cooling rate during solidification. If the dendrite arm spacing can be established in this manner, a comprehensive set of models would exist allowing for an informed choice of processing parameters during solidification, homogenization, and γ-quenching in U-Mo alloy castings of arbitrary dimensions; ensuring uniformity and inhibiting formation of the detrimental α-phase. Thermal models based upon computational fluid dynamics and thermodynamic data can provide spatially specific temperature profiles during solidification for U-Mo [21], from which dendrite arm spacing and solute segregation could then be derived. From this known microstructure, homogenization holds [12–15] and/or cooling rates necessary to quench in the y-phase through the eutectoid without forming equilibrium [5, 6] or metastable phases [7] can be predicted.

4. Conclusions

The Brody-Fleming model, which accounts for limited diffusion in the solid phase, is able to replicate experimental solute segregation profiles that cannot be modeled by the simpler case of Scheil cooling. This model can be used to make informed choices considering the effects of cooling rate on solute segregation and to help predict the necessary length of subsequent homogenization processes. The findings highlight the need for further studies establishing the relationship between dendrite size, composition, and cooling rate in the U-Mo system. With a complementary model for dendrite formation, the solute segregation model allows for a complete prediction of the microstructure at each volume element as a function of cooling rate and composition.

Acknowledgments

The authors would like to thank Vineet Joshi, Pacific Northwest National Laboratory, for valuable discussions and his help identifying pertinent resources.

Funding for this research was provided by the Y-12 National Security Complex's Plant Directed Research and Development program. This work of authorship and those incorporated herein were prepared by Consolidated Nuclear Security, LLC (CNS) Pantex Plant/Y-12 National Security Complex as accounts of work sponsored by an agency of the United States Government under contract DE NA0001942. Neither the United States Government nor any agency thereof, nor CNS, nor any of their employees, makes any warranty, express or implied, or assumes any legal liability or responsibility for the accuracy, completeness, use made, or usefulness of any information, apparatus, product, or process disclosed, or represents that its use would not infringe privately owned rights. Reference herein to any specific commercial product, process, or service by trade name, trademark, manufacturer, or otherwise, does not necessarily constitute or imply its endorsement, recommendation, or favoring by the United States Government or any agency or contractor thereof, or by CNS. The views and opinions of authors expressed herein do not necessarily state or reflect those of the United States Government or any agency or contractor thereof, or by CNS. This document has been authored by CNS LLC, a contractor of the U.S. Government under contract DE NA0001942, or a subcontractor thereof. Accordingly, the U.S. Government retains a paid up, nonexclusive, irrevocable, worldwide license to publish or reproduce the published form of this contribution, prepare derivative works, distribute copies to the public, and perform publicly and display publicly, or allow others to do so, for U. S. Government purposes.

Appendix A. Converting compositional maps to solute segregation profiles

Data relating to solute segregation is typically presented as a concentration map. In order to convert this map into a solute segregation profile as a function of solidification, it must first be converted into a cumulative distribution function (CDF) of areal fraction as a function of composition. In the case of U-Mo, it is most convenient to place Mo concentration in decreasing order along the abscissa, with the ordinate axis being the fraction of the concentration map area at or above that concentration (so that the CDF rises from 0 to 1). As volume elements with less solute will always have solidified later in the freezing process, if the CDF is constructed in this manner all that is necessary to produce a solute segregation profile is to flip the two axes and relabel the cumulative percentage as the solidified fraction.

If an original data file for the concentration map is not available, but the map is obtainable in image form, it is still possible to manually construct a CDF in order to compute the solute segregation profile. If presented as a color map or grayscale image there are numerous image analysis software packages available that allow for the number of pixels within a defined color/intensity range to be counted (e.g. color thresholding in freeware ImageJ [22]). From these pixel counts (which scale to areal fraction) a CDF can be constructed. If the concentration map is available only in the format of contoured lines, such as Ref. [7], we advise that an image editor be used to fill each contour level in with a unique color value; after which the contour map can be analyzed in a similar fashion to a color map.

References

[1] E. Nyberg, D. Paxton, V. Joshi, D. Burkes, C. Lavender, The Influence of Casting Conditions on the Microstructure of As-Cast U-10Mo Alloys: Characterization of the Casting Process Baseline, Pacific Northwest Nation Lab, PNNL-23049, 2013.
[2] F. Rough, A. Bauer, Constitution of Uranium and Thorium Alloys, BMI-1300, Battelle Memorial Institute, 1958, p. 41.
[3] T. Massalski, H. Okamoto, P. Subramanian, L. Kacprzak, Binary Alloy Phase Diagram, second ed., ASM International, Materials Park, OH, 1990.
[4] J.E. Burke, A.M. Turkalo, The Growth of Uranium upon Thermal Cycling, 50, Transactions of the ASM, 1957, pp. 943–953.
[5] N. Peterson, S. Rothman, Diffusion in Gamma Uranium, Phys. Rev. 136 (1964) 842–848.
[6] W. Bostrom, M. Burkart, E. Halteman, R. Leggett, R. McGeary, T. Padden, Development and Properties of Uranium-Base Alloys Corrosion Resistance in High Temperature, Westinghouse Electric Corp. Atomic Power Div., Pittsburgh, 1955.
[7] T. Pedrosa, A.D. Santos, F. Lameiras, P. Cetlin, W. Ferraz, Phase transitions during artificial ageing of segregated as-cast U–Mo, J. Nucl. Mater. 457 (2015) 100–117.
[8] H. Brody, M. Flemings, Solute redistribution in dendritic solidification, Trans. Met. Soc. AIME 236 (1966) 615–624.
[9] R. Cahn, P. Hassen, Chapter 8, Section 6: Solidification of alloys with planar and nearly planar S-L interfaces, in: Physical Metallurgy, fourth ed., 1996, pp. 714–718. North Holland.
[10] D. Stefanescu, Chapter 5: Diffusive Mass Transport at the Macroscale, in: Science and Engineering of Casting Solidification, third ed., Springer, 2015, pp. 67–88.
[11] S. Kobayashi, Solute redistribution during solidification with diffusion in solid phase: A theoretical analysis, J. Cryst. Growth 88 (1988) 87–96.
[12] E. Nyberg, D. Paxton, V. Joshi, D. Burkes, C. Lavender, Influence of Homogenization on the Mechanical Properties and Microstructure of the U-10Mo

Alloy, Pacific Northwest National Lab, PNNL-23348, 2014.
[13] V.V. Joshi, E.A. Nyberg, C.A. Lavender, D. Paxton, D.E. Burkes, Thermo-mechanical process optimization of U-10wt% Mo Part 2: The effect of homogenization on the mechanical properties and, J. Nucl. Mater. 465 (2010) 710–718.
[14] Z. Xu, V. Joshi, S. Hu, D. Paxton, C. Lavender, D. Burkes, Modeling the Homogenization Kinetics of As-Cast U-10 wt% Mo Alloys, Pacific Northwest National Laboratory, PNNL-24145, 2015.
[15] Z. Xu, V. Joshi, S. Hu, D. Paxton, C. Lavender, D. Burkes, Modeling the Homogenization Kinetics of As-Cast U-10wt% Mo alloys, J. Nucl. Mater. 10 (2016), 1016/j.jnucmat.2015.11.026.
[16] E. Scheil, Bemerkungen zur schichtkristallbildung, Z. für Met. 34 (1942) 70.
[17] Y. Adda, A. Kirianenko, Etude de L'Autodiffusion de L'Uranium en Phase γ, J. Nucl. Mater. 1 (1962) 120–126.
[18] Y. Adda, A. Kirianenko, Abaissement des Coefficients D'Autodiffusion de L'Uranium en Phase γ par des Additions de Molybdene, de Zirconium ou de Niobium, J. Nucl. Mater. 6 (1) (1962) 135–136.
[19] K. Huang, D. Miller, Y. Sohn, Interdiffusion, Intrinsic Diffusion, Atomic Mobility, and Vacancy Wind Effect in Gamma(BCC) Uranium-Molybdenum Alloy, Met. Trans. A 44 (2013) 738–746.
[20] E. Nyberg, D. Paxton, V. Joshi, D. Burkes, C. Lavender, The Influence of Casting Conditions on the Microstructure of As-Cast U-10Mo Alloys: Characterization of the Casting Process Baseline, Pacific Northwest Nation Lab, PNNL-23049, 2013.
[21] R. Aikin, D. Dombrowski, Progress in Optimization of U-10Mo Fuel Casting by Modeling and Experiment, in: Transactions of the European Reasearch Reactor Conference, 2014, pp. 188–197.
[22] W. Rasband, ImageJ, U. S. National Institutes of Health, Bethesda, Maryland, USA, 1997-2016 [Online]. Available, http://imagej.nih.gov/ij/.